

Conformal mappings and shape derivatives for the transmission problem with a single measurement.

Lekbir Afraites*

Marc Dambrine*

Djalil Kateb*

March 7, 2006

Abstract

In the present work, we consider the inverse conductivity problem of recovering inclusion with one measurement. First, we use conformal mapping techniques for determining the location of the anomaly and estimating its size. We then get a good initial guess for quasi-Newton type method. The inverse problem is treated from the shape optimization point of view. We give a rigorous proof for the existence of the shape derivative of the state function and of shape functionals. We consider both Least Squares fitting and Kohn and Vogelius functionals. For the numerical implementation, we use a parametrization of shapes coupled with a boundary element method. Several numerical examples indicate the superiority of the Kohn and Vogelius functional over Least Squares fitting.

Keywords inverse conductivity problem, shape optimization, shape derivatives, conformal mappings, boundary element methods.

AMS 49K20, 49N60, 49Q10, 30C30, 65N38.

1 Introduction

We consider the inverse conductivity problem with one measurement of recovering, within a bounded domain $\Omega \subset \mathbb{R}^2$ whose conductivity is σ_1 , an unknown inclusion ω in Ω of conductivity $\sigma_2 \neq \sigma_1$ by measuring on $\partial\Omega$, the input voltage and the corresponding output current. In the sequel, we fix $d_0 > 0$ and consider inclusions ω such that $\omega \subset\subset \Omega_{d_0} = \{x \in \Omega, d(x, \partial\Omega) > d_0\}$. To set up the problem, we consider a conducting body occupying $\Omega \subset \mathbb{R}^2$ with a conductivity

$$\sigma = \sigma_1 \chi_{\Omega \setminus \omega} + \sigma_2 \chi_{\omega}, \quad \sigma_1, \sigma_2 > 0 \tag{1}$$

where ω is a simply connected subdomain of Ω . The notation χ_{ω} (resp. $\chi_{\Omega \setminus \omega}$) denotes the characteristic function of ω (resp. $\Omega \setminus \omega$). Then if the electrostatic potential u solves

$$-\operatorname{div}(\sigma \nabla u) = 0 \text{ in } \Omega, \tag{2}$$

*Laboratoire de Mathématiques Appliquées de Compiègne, Université de Technologie de Compiègne

one wishes to recover ω from the knowledge of the boundary voltage f and current measurements g whose relationship is determined by the following equation

$$\begin{cases} -\operatorname{div}(\sigma \nabla u) &= 0 \text{ in } \Omega, \\ u &= f \text{ on } \partial\Omega, \\ \sigma_1 \partial_n u &= g \text{ on } \partial\Omega. \end{cases} \quad (3)$$

Here $\partial_n u$ denotes the normal derivative of u . This inverse problem arises in practical situations, such as medical imaging, exploration geophysics and non-destructive evaluation where measurements made on the exterior of a body are used to deduce the properties of the hidden interior and inclusions. The fundamental question of existence and uniqueness of a solution to the inverse problem is non trivial and no general answer is known to our best knowledge. The difficulty lays in the single measurement condition. However, we are not dealing with this question in this work but with the design of numerical techniques to effectively reconstruct the interface $\partial\omega$.

Our work is the natural continuation of the paper [4] where we introduced an algorithm based on the use of conformal mapping to efficiently reconstruct circular inclusions in tomography. The leading idea is to consider the conformal map itself as variable and the analytic expression of the Dirichlet to Neumann map in the case of concentric disks. Such techniques were introduced by Kress and al in [1], [6] where they considered the particular cases of the perfectly conducting or insulating inclusions. However, the extension of the conformal mapping methods to the general transmission case requires to consider only circular inclusions. This limitation is intrinsic to the use of conformal mapping of doubly connected domains. Therefore, the natural question is : how useful are those conformal mapping methods when one deals with inclusions far from being circular? Our aim in this paper is to give a simple answer: we can use this method for determining the location and an estimated size of the inclusion. We will then get a good initial guess that will be incorporated in a more complex algorithm. This algorithm can be summarized as follows: first, thanks to the conformal mapping, we begin to find an admissible approximating disk; in a second time we choose a criterion and use a quasi-Newton procedure to minimize this criterion. Let us emphasize that the unknown is a geometry and therefore we are facing a shape optimization problem.

We consider different criteria such as the Least-Squares boundary fitting criterion and the Kohn-Vogelius criterion and solve the corresponding minimization problems by an optimization method. We discretize the continuous gradient of the objectives. From the numerical results obtained with quasi-Newton algorithms such as BFGS, we will be able to determine which criterion is more suited for our problem.

The organization of the paper follows the objective. In a first section, we shortly present the conformal mapping techniques from a practical point of view. We also give some comments on the convergence conditions of the algorithm and derive an *a priori* upper bound for the conformal radius. In the second section, we derive the shape calculus for the solution of equation (2). Since we have to differentiate the energy functionals with respect to the variations of the boundary, the knowledge of the shape derivative of the state equation with respect to the boundary variations is required for an efficient implementation of an optimization method. We will introduce the shaping functions and will compute their shape derivatives. In the last part of the paper, we introduce a discretization of the problem based on the discretization of the continuous gradients. In order to compute the gradients, we introduce some systems of integral equations and prove their well-posedness. This will enable us to use a classical optimization method to improve the quality of the reconstruction. We will illustrate our theoretical results with several numerical examples obtained with the criteria we previously introduced.

2.1 Presentation of the algorithm of [4] and convergence results

To simplify many expressions in this section, we assume from now on that the known domain Ω is the unit disk $B(O, 1)$ and that the inclusion is a disk $\omega \subset\subset \Omega_{d_0}$. There exists a radius ρ and a Möbius transform Ψ mapping Ω into itself and ω into $B(o, \rho)$.

In order to perform the transport, we need some notations: let Γ be a periodic parametrization of $\partial\Omega$ by the arc length. From now on we consider $\Phi = \Psi^{-1}$, the conformal mapping transforming the concentric circles onto $\partial\Omega$ and $\partial\omega$. We normalize the mapping Φ by setting $\Phi(1) = \Gamma(0)$. If the circle $\partial\Omega$ is parameterized by $\partial\Omega = \{\theta(t) = e^{it}, t \in [0, 2\pi]\}$, then we can find a strictly monotonous and smooth bijection ϕ such that $\Phi \circ \theta = \Gamma \circ \phi$; ϕ is the main determination of the argument of $\Phi(e^{it})$. If u is an harmonic function in a neighborhood of $\partial\Omega$ and if $v = u \circ \Phi$ then applying the chain rule and the Cauchy-Riemann relations we get

$$\frac{\partial v}{\partial n} = \frac{\partial u}{\partial \nu} \frac{d\phi}{dt} \text{ on } \partial\Omega. \quad (4)$$

Since the state function u solves (3), we get

$$\mathcal{D}_\rho(f \circ \phi) = \frac{d\phi}{dt} g \circ \phi \text{ on } \partial\Omega, \quad (5)$$

where \mathcal{D}_ρ denotes the Dirichlet to Neumann operator and f and g depend on the arclength of $\partial\Omega$. In the specific case of two concentric disks of radii ρ and 1, \mathcal{D}_ρ is explicitly known.

Lemma 2.1 *The operator \mathcal{D}_ρ is diagonal on the Fourier basis:*

$$\mathcal{D}_\rho \left(\frac{1}{\sqrt{\pi}} \begin{bmatrix} \cos k\theta \\ \sin k\theta \end{bmatrix} \right) = \lambda_k \left(\frac{1}{\sqrt{\pi}} \begin{bmatrix} \cos k\theta \\ \sin k\theta \end{bmatrix} \right) \text{ with } \lambda_k(\rho) = \sigma_1 k \frac{1 - \mu\rho^{2k}}{1 + \mu\rho^{2k}}. \quad (6)$$

In these formulae, μ is the relative contrast of conductivities namely $(\sigma_1 - \sigma_2)/(\sigma_1 + \sigma_2) \in (-1, 1)$.

The unknowns in (5) are ρ and ϕ . When ρ is a real number between 0 and 1, ϕ is a 2π -periodic function. Equation (6) provides the radius ρ from the eigenvalues λ_k by

$$\forall k \neq 0, \quad \rho = \left| \frac{\sigma_1 k - \lambda_k}{\mu(\sigma_1 k + \lambda_k)} \right|^{\frac{1}{2k}} \quad (7)$$

Hence, once ϕ is fixed, the eigenvalues of \mathcal{D}_ρ are recovered from the projections of $f \circ \phi$ and $g \circ \phi$ on the eigensubspaces of \mathcal{D}_ρ . This means that in practise the only unknown is ϕ . The equation (5) is nonlinear and nonlocal. The computational and theoretical way to solve such an equation was introduced by Akduman and Kress in [1]: it consists in writing this equation as a fixed point for a contractant nonlinear operator K . In order to prove contraction, a linearization is performed and the measurements f and g have to be properly chosen. These limitations explain the limitation of the results in [1], [6], [4]. We now introduce the appropriate operator K for the transmission problem. The full analysis is carried out in [4].

To avoid division by 0, equation (5) is rewritten in a relaxed form

$$\frac{d\phi}{dt} = \frac{(g \circ \phi)\mathcal{D}_\rho[f \circ \phi] + (G \circ \phi)\mathcal{D}_0[F \circ \phi]}{(g^2 + G^2) \circ \phi}. \quad (8)$$

The couple (F, G) satisfies the following compatibility with the measurements condition : *there exists a function G with mean value 0 in $L^2(\partial\Omega)$ such that $g^2 + G^2 \geq \gamma$ holds for some $\gamma > 0$ on $\partial\Omega$* . The function F is then taken as the trace on $\partial\Omega$ of a solution to the Neumann problem $-\Delta w = 0$ in Ω with $\partial_n w = G$ on $\partial\Omega$. However, they can be seen as simulated data for the reference problem without inclusion.

Let us introduce the operators V, U and K defined as

$$V : H^1(0, 2\pi) \rightarrow H^1(0, 2\pi)$$

$$\psi \mapsto \psi(t) + t.$$

$$U : H^1(0, 2\pi) \rightarrow L^2(0, 2\pi)$$

$$\psi \mapsto \frac{(g \circ V\psi)\mathcal{D}_\rho[f \circ V\psi] + (G \circ V\psi)\mathcal{D}_0[F \circ V\psi]}{(g^2 + G^2) \circ V\psi}. \quad (9)$$

$$K : H^1(0, 2\pi) \rightarrow H^1(0, 2\pi)$$

$$\psi \mapsto \int_0^t \left(U\psi(x) - \frac{1}{2\pi} \int_0^{2\pi} U\psi(\tau) d\tau \right) dx. \quad (10)$$

We have :

Theorem 2.2 ([4]) *Assume that $\Omega \setminus \bar{\omega}$ is close to an annulus bounded by concentric circles with an inner radius ρ and that the pair of measures (f, g) are close to a sine function. If $\sigma_2 > \sigma_1$ and the condition*

$$\frac{-\mu\rho^2(1-\rho^2)^2}{(1-\mu\rho^2)(1+\mu\rho^4)^2} - \frac{4\mu\rho^2}{1-\mu\rho^2} \left[\frac{1}{5} + \frac{1}{3} \frac{1-\rho^2}{1+\mu\rho^2} \right] < \frac{1-\rho^2}{1+\mu\rho^4}, \quad (11)$$

holds then the inclusion ω can be reconstructed via iterative approximations $\psi_{n+1} = K(\psi_n)$. Moreover, if (F, G) is a second measurement, then condition (11) can be removed.

Two assumptions limit the field of application of this method. Let us make some comments about these restrictions.

The condition $\sigma_2 > \sigma_1$ - the conductivity in the inclusion should be bigger than the conductivity outside - is intriguing. Technically, if $\sigma_2 < \sigma_1$, K has an eigenvalue strictly bigger than 1 and is not contracting. In that case, we can consider the corresponding problem for v an harmonic conjugate function of the state u . It solves classically

$$\begin{cases} -\operatorname{div}(\tilde{\sigma}\nabla v) & = 0 \text{ in } \Omega, \\ v & = g \text{ on } \partial\Omega, \\ \tilde{\sigma}_1\partial_n v & = \frac{df}{ds} \text{ on } \partial\Omega. \end{cases}$$

where $\tilde{\sigma}$ is the inverse of σ and s stands for the arc-length of $\partial\Omega$. The conjugate harmonic function is defined by (3) up to an additive constant. Obviously, the points of discontinuity of $\tilde{\sigma}$ are ω and one checks that $\tilde{\sigma}_2 > \tilde{\sigma}_1$. If f and g are regular enough to apply the same strategy for the new set of data (g, f') , we are led to study the operator \tilde{K} defined by

$$\tilde{U} : H^1(0, 2\pi) \rightarrow L^2(0, 2\pi)$$

$$\psi \mapsto \frac{(f' \circ V\psi)\mathcal{D}_\rho[g \circ V\psi] + (G \circ V\psi)\mathcal{D}_0[F \circ V\psi]}{(f'^2 + G^2) \circ V\psi}. \quad (12)$$

$$\tilde{K} : H^1(0, 2\pi) \rightarrow H^1(0, 2\pi)$$

$$\psi \mapsto \int_0^t \left(\tilde{U}\psi(x) - \frac{1}{2\pi} \int_0^{2\pi} \tilde{U}\psi(\tau) d\tau \right) dx.$$

It is an exercise to adapt the study of K performed in [4] to show that in this case, \tilde{K} is also not contracting. This means that the constraint $\sigma_2 > \sigma_1$ cannot be removed in this way.

The other restriction is the size condition (11): the key quantity $\mu\rho^2$ -namely the product of the conductivity contrast by the area of the conformal inclusion- should not be too big. Since μ is known by assumption, we are led to the question of obtaining *a priori* bounds on the conformal radius ρ from effective data. They correspond, in the context of conformal mapping, to the general results of *a priori* estimations of size.

2.2 Size estimations of the conformal radius

The size estimate is comparable with the boundary integral

$$\delta\mathcal{E} = \int_{\partial\Omega} g(f - f_0) dS$$

where f_0 denotes the Dirichlet data for g , when we have no inclusion (see for example [11],[2]). If Λ_0^{-1} is the Neumann-to-Dirichlet map associated with the Laplace operator on $B(0,1)$, then $f_0 = \Lambda_0^{-1}g$. Here $\delta\mathcal{E}$ represents the difference between the energy powers \mathcal{E} and \mathcal{E}_0 when the inclusion is respectively present and absent. Before giving an estimation of the size of the radius, some preliminaries are needed. We assume that ω is a disk of center $a \in B(0,1 - d_0)$ and of unknown radius. Concerning the boundary measurement, we make the assumption that the Neumann data g is steep when it is small:

(A) *There exists a number $M > 0$ such that when $|g(x)| < M$ then its derivative satisfies*

$$|g'(x)| > \frac{12}{d_0^5} M.$$

This assumption plays the same role than assumption (N1) of [11]. Our size estimation of the conformal radius ρ is given by the following result.

Proposition 2.3 *Assume that g satisfies (A). There exists a constant $C > 0$, depending only on the conductivities σ_1, σ_2 , such that*

$$\rho^2 \leq \frac{C}{\pi M^2} \left| \int_{\partial\Omega} (g - g_0) f \, dx \right|. \quad (13)$$

Proof: By the Möbius transform

$$\Phi(z) = \frac{z - a}{1 - \bar{a}z},$$

we transport the problem on the configuration of an annulus of inner radius ρ . Since the trace of Φ on the boundary $\partial\Omega$ writes:

$$e^{i\phi(\theta)} = e^{-i\theta} \frac{(e^{i\theta} - a)^2}{|e^{i\theta} - a|^2},$$

a straightforward computation leads to

$$\phi'(t) = \frac{1 - |a|^2}{1 + |a|^2 - 2x_a \cos t - 2y_a \sin t} \geq \frac{1 - |a|}{1 + |a|} \geq \frac{d_0}{2}$$

and $|\phi''(t)| \leq 2 \frac{|a|(1 + |a|)}{(1 - |a|)^3} \leq \frac{2}{d_0^3}.$

The transported boundary conditions are $\tilde{f} = f \circ \phi$ and $\tilde{g} = (g \circ \phi)\phi'$. Hence, we have on the one hand

$$\int_{\partial\Omega} (f - f_0)g = \int_{\partial\Omega} (\tilde{f} - \tilde{f}_0)\tilde{g},$$

on the other hand, $|\tilde{g}(x)| < M \Rightarrow |\tilde{g}'| > M$. Then, from Theorems 3.1 (size estimate) and 4.1 (lower bound for the norm of the gradient) of [11], there exists a constant $C > 0$ depending only of the conductivities σ_1, σ_2 such that

$$\rho^2 \leq \frac{C}{\pi M^2} \left| \int_{\partial\Omega} (f - f_0)g \right|.$$

■

Our result should be useful in practice: indeed, we have a decision tool for the convergence of the fixed point that needs only the boundary measurements and conductivity.

2.3 The numerical algorithm

The function ψ is approximated in E_d the subspace of trigonometric polynomials of order less than d . The known and fixed data are the measurements f, g , the *virtual* measurements F, G and the conductivities. We assume that both the contrast of conductivity and the spectra of \mathcal{D}_0 are computed once for all. Let us first explain how to apply numerically the fixed point operator. Assume that the approximations ρ_n and ψ_n are known after n iterations. Two main steps are to be performed.

1. *Step 1: computation of the new fonction ψ_{n+1} .*
 - (a) determine the eigenvalues of \mathcal{D}_{ρ_n} ,
 - (b) compute $f \circ \phi_n, g \circ \phi_n, F \circ \phi_n$ and $G \circ \phi_n$, (this requires numerical interpolation)
 - (c) compute the Fourier coefficients of $f \circ \phi_n$ and $g \circ \phi_n$,
 - (d) compute U pointwise according to (9),
 - (e) compute the Fourier coefficients of U and deduce ψ_{n+1} ,
 - (f) set $\phi_{n+1}(t) = t + \psi_{n+1}(t)$;
2. *Step 2: computation of the new radius ρ_{n+1} .*
 - (a) compute the Fourier coefficients α_k of $\phi'_{n+1} g \circ \phi_{n+1}$ and β_k of $f \circ \phi_{n+1}$,
 - (b) determine $k_0 = \min\{k, |\beta_k|^2 + |\beta_{-k}|^2 \neq 0\}$,
 - (c) evaluate $\lambda = \sqrt{(|\alpha_{k_0}|^2 + |\alpha_{-k_0}|^2)/(|\beta_{k_0}|^2 + |\beta_{-k_0}|^2)}$,
 - (d) determine ρ_{n+1} from (7).

The main advantage of this algorithm is that no partial differential equation and no linear system has to be solved. Hence, it is fast and cheap. Once convergence is achieved, one disposes of a numerical approximation $\tilde{\phi}$ of ϕ and of an approximation $\tilde{\rho}$ of the radius ρ . It remains to extend $\tilde{\phi}$ into a conformal map in the disk. Theoretically, this is performed as follows: if $\tilde{\phi}$ writes

$$\tilde{\phi}(t) \approx \sum_{k=1}^N a_k \cos kt + b_k \sin kt = \sum_{k=1}^N \frac{a_k - ib_k}{2} e^{ikt} + \sum_{k=1}^N \frac{a_k + ib_k}{2} e^{-ikt}.$$

Then its extension is

$$\tilde{\Phi}(re^{it}) \approx \sum_{k=1}^N \frac{a_k - ib_k}{2} r^k e^{ikt} + \sum_{k=1}^N \frac{a_k + ib_k}{2} r^{-k} e^{-ikt}.$$

The ill-posedness of the problem appears in the negative exponent of r . Hence, we use the regularized conformal mapping Φ_r :

$$\Phi_r(re^{it}) \approx \sum_{k=1}^N \frac{a_k - ib_k}{2} r^k e^{ikt} + \sum_{k=1}^N \frac{a_k + ib_k}{2} \frac{r^k}{\varepsilon_k + r^{2k}} e^{-ikt}.$$

In the numerical results presented in Section 4, we arbitrarily fix the Tychonov parameters ε_k .

3 Shape calculus and transmission problem

3.1 Reformulation as shape optimization problems

In parameter identification, one usually tries to fit the data with the predicted output generated by the model from a given value of the parameter. Hence, we define the Neumann Least Squares fitting cost function as

$$J_{LS}(\omega) = \frac{1}{2} \int_{\partial\Omega} |\sigma_1 \partial_n u_d - g|^2. \quad (14)$$

where g is the boundary measurement and where the state function u_d solves

$$\begin{cases} \Delta u_d &= 0 \text{ in } \Omega \setminus \bar{\omega} \text{ and in } \omega, \\ [u_d] &= 0 \text{ on } \partial\omega, \\ [\sigma \partial_n u_d] &= 0 \text{ on } \partial\omega, \\ u_d &= f \text{ on } \partial\Omega. \end{cases} \quad (15)$$

The problem of determining the inclusion ω is now to minimize this shape function. A similar functional is also considered in [12] for interior fitting. Since we consider L^2 norm we assume that the boundary $\partial\Omega$ is of class \mathcal{C}^2 and that the Dirichlet data f is $H^{3/2}$ to insure that J_{LS} is well defined. To avoid this artificial difficulty, one usually prefers to fit Dirichlet data rather than Neumann data. In that case, we have

$$J_{DLS}(\omega) = \frac{1}{2} \int_{\partial\Omega} |u_n - f|^2,$$

where u_n solves

$$\begin{cases} \Delta u_n &= 0 \text{ in } \Omega \setminus \bar{\omega} \text{ and in } \omega, \\ [u_n] &= 0 \text{ on } \partial\omega, \\ [\sigma \partial_n u_n] &= 0 \text{ on } \partial\omega, \\ \partial_n u_n &= g \text{ on } \partial\Omega. \end{cases} \quad (16)$$

To insure uniqueness, we impose the normalization condition

$$\int_{\partial\Omega} u_n = \int_{\partial\Omega} f. \quad (17)$$

While Least Squares fitting criteria as J_{LS} are widely used in the literature of inverse problems, a Kohn-Vogelius criterion has to our best knowledge been used only for the simpler case of perfectly conducting inclusions (see [13] and [5]). In general, those functionals are expected to lead to more robust optimization procedures. In the context of the transmission problem, we define the Kohn-Vogelius cost function as

$$J_{KV}(\omega) = \int_{\Omega} \sigma |\nabla(u_d - u_n)|^2. \quad (18)$$

It measures the gap of energy between the solutions of the Dirichlet and Neumann problem corresponding to the data. This function is positive and vanishes only if $u_d = u_n$ which is the case when the parameter ω fits

the inclusion. We first give a boundary expression of J_{KV} . By integration by parts and the jump condition⁸ on $\partial\omega$, we have:

$$\begin{aligned} J_{KV}(\omega) &= \int_{\Omega \setminus \bar{\omega}} \sigma_1 |\nabla(u_d - u_n)|^2 + \int_{\omega} \sigma_2 |\nabla(u_d - u_n)|^2, \\ &= \int_{\partial\Omega} (\sigma_1 \partial_n u_d - g)(f - u_n) + \int_{\partial\omega} [\sigma \partial_n(u_d - u_n)](u_d - u_n), \\ &= \int_{\partial\Omega} (\sigma_1 \partial_n u_d - g)(f - u_n). \end{aligned}$$

To define and compute the continuous gradients of these functionals, we use the classical shape calculus developed by Murat-Simon and others. We refer to the book [8] for all the general explanations on how to differentiate with respect to the shape.

3.2 Derivatives of the state functions

Let us first fix the notations. We set $n_{\partial\omega}$ the unit normal vector to $\partial\omega$ pointing into $\Omega \setminus \bar{\omega}$; hence $\partial_n u^-$ means the limit of the normal derivative seen from the inside of ω . Let V denote a smooth vector field with compact support in Ω_{d_0} and we set $V_n = \langle V, n_{\partial\omega} \rangle$ its normal component. In the sequel, the tangential gradient is denoted by ∇_τ and the tangential divergence by div_τ . We set $\Phi_t(x) = x + tV(x)$, this transformation is as smooth as V and for small t is invertible. We also set

$$A(t, x) = D\Phi_t^{-1}(x)^t D\Phi_t^{-1}(x) \det D\Phi_t(x).$$

We recall some classical facts in shape optimization: $A(t, x)$ is symmetric positive and for $t < t_0$ one has $y^t A(t, x) y \geq \|y\|^2/2$, moreover A is a smooth application (it depends only on V) with $A(0, x) = I$ and

$$\mathcal{A} = \frac{d}{dt} A(t, x)|_{t=0} = \text{div}(V) I - (DV^t + DV).$$

Theorem 3.1 *The state u_d has a material derivative $\dot{u}_d \in H_0^1(\Omega)$ that solves*

$$\forall v \in H_0^1(\Omega), \quad \langle \sigma \nabla \dot{u}_d, \nabla v \rangle = -\langle \sigma \mathcal{A} \nabla u_d, \nabla v \rangle. \quad (19)$$

The state u_d is shape differentiable and its shape derivative u' satisfies

$$\left\{ \begin{array}{l} \Delta u'_d = 0 \text{ in } \Omega \setminus \bar{\omega} \text{ and in } \omega, \\ [u'_d] = \frac{\sigma_1 - \sigma_2}{\sigma_1} \partial_n u_d^- V_n \text{ on } \partial\omega, \\ [\sigma \partial_n u'_d] = (\sigma_1 - \sigma_2) \text{div}_\tau (V_n \nabla_\tau u_d) \text{ on } \partial\omega, \\ u'_d = 0 \text{ on } \partial\Omega. \end{array} \right. \quad (20)$$

Before proving this result, we have to make some comments. If we assume that the state u_d is shape differentiable, we formally obtain (20) by differentiation of the jump conditions. The most notable point is the jump condition for the derivative u'_d : it does not vanish. This means that the derivative u'_d is not continuous across the interface $\partial\omega$. As a consequence, u'_d cannot belong to $H^1(\Omega)$, it belongs only to $H^1(\Omega \setminus \bar{\omega}) \cup H^1(\omega)$. A more precise analysis is required. In [9], formula (20) was first derived. We find it useful to explain how both existence of the derivative and (20) can be obtained by the classical methods of shape optimization. Hence we give a complete proof of Theorem 3.1 and show that the material derivative belongs to $H_0^1(\Omega)$.

Proof: We decompose the proof in the four classical parts: first transport the problem on a fixed domain⁹, then prove weak convergence to the material derivative, then strong convergence and return to the shape derivative.

First step. In order to work with homogeneous Dirichlet conditions, we introduce \check{f} an $H^1(\Omega)$ extension of f with support in Ω_{d_0} . Let $u_d(t)$ denote the solution of (15) with inclusion $\omega(t) = \Phi_t(\omega)$ and $w(t) = u_d(t) - \check{f} \in H_0^1(\Omega)$. Then, the transported $\tilde{w}(x) = w(t, \Phi_t(x))$ solves the variational equation:

$$\forall v \in H_0^1(\Omega), \quad \int_{\Omega} \sigma A(t, x) \nabla \tilde{w}(x) \nabla v(x) = - \int_{\Omega} \sigma \nabla \check{f} \nabla v.$$

Second step. Subtracting the variational equation solved by $w_0 = u_d - \check{f}$, we obtain:

$$\forall v \in H_0^1(\Omega), \quad \langle \sigma A(t) \frac{\nabla \tilde{w} - \nabla w_0}{t}, \nabla v \rangle = \langle \sigma \frac{I - A(t)}{t} \nabla w_0, \nabla v \rangle. \quad (21)$$

Plugging $\tilde{w} - w_0$ as test function, we get by the properties of A

$$\frac{1}{2} \min(\sigma_1, \sigma_2) \left\| \frac{\nabla \tilde{w} - \nabla w_0}{t} \right\|_{L^2(\Omega)} \leq \left\| \frac{A(t, x) - I}{t} \right\|_{\infty} \|\nabla w_0\|_{L^2(\Omega)}.$$

Therefore $(\tilde{w} - w_0)/t$ is bounded in $H_0^1(\Omega)$. Hence the sequence is weakly convergent in H_0^1 and its weak limit is the material derivative \dot{u}_d of u .

Third step. We show the strong convergence of $(\tilde{w} - w_0)/t$. Passing to the limit $t \rightarrow 0$ in (21), we check that \dot{u}_d solves

$$\langle \sigma \nabla \dot{u}_d, \nabla v \rangle = - \langle \sigma \mathcal{A} \nabla w_0, \nabla v \rangle.$$

This was stated as (19) in Theorem 3.1 where w_0 was changed in u_d thanks to the support of \mathcal{A} . This information enables us to show the strong convergence in $H_0^1(\Omega)$; indeed setting $v = (\tilde{w} - w_0)/t$ in (21), we get

$$\langle \sigma A(t) \nabla v, \nabla v \rangle = \langle \sigma \frac{I - A(t)}{t} \nabla w_0, \nabla v \rangle = E_{1,t} + E_{2,t} \quad (22)$$

where

$$E_{1,t} = \langle \sigma (A(t) - I) \nabla v, \nabla v \rangle, \quad \text{and} \quad E_{2,t} = \langle \sigma \left(\frac{I - A(t)}{t} \right) \nabla \tilde{w}, \nabla v \rangle.$$

The weak convergence of $(\tilde{w} - w_0)/t$ leads after straightforward calculations to

$$E_{1,t} \rightarrow 0 \quad \text{and} \quad E_{2,t} \rightarrow - \langle \sigma \mathcal{A} \nabla w_0, \nabla \dot{u}_d \rangle \quad \text{when} \quad t \rightarrow 0.$$

By (19), we conclude that $E_{2,t} \rightarrow \langle \sigma \nabla \dot{u}_d, \nabla \dot{u}_d \rangle$. This shows that ∇v converges strongly to $\nabla \dot{u}_d$ in $L^2(\Omega)$. From Poincaré's inequality, we deduce the strong convergence of v to \dot{u}_d in $H_0^1(\Omega)$.

Fourth Step. We deduce the equations satisfied by the shape derivative $u'_d = \dot{u}_d - h \cdot \nabla u_d$.

Set $b = (h \cdot \nabla u) \nabla v + (h \cdot \nabla v) \nabla u - (\nabla u \cdot \nabla v) h$. We will use the classical identity

$$- \nabla u \cdot \mathcal{A} \nabla v = \operatorname{div}(b) - (h \cdot \nabla u) \Delta v - (h \cdot \nabla v) \Delta u. \quad (23)$$

From the identity satisfied by \dot{u}_d , we have

$$\int_{\Omega} \sigma \nabla \dot{u}_d \cdot \nabla v = \int_{\Omega} \sigma \operatorname{div}(b) - \int_{\Omega} \sigma (h \cdot \nabla u_d) \Delta v - \int_{\Omega} \sigma (h \cdot \nabla v) \Delta u_d, \quad (24)$$

from the divergence theorem and after an integration by parts, we get

$$\int_{\Omega} \sigma \nabla \dot{u}_d \cdot \nabla v = - \int_{\partial \omega} [\sigma (h \cdot \nabla v) \partial_n u_d] + \int_{\partial \omega} [\sigma (\nabla u_d \cdot \nabla v) h_n] + \int_{\Omega} \sigma \nabla (h \cdot \nabla u_d) \nabla v.$$

Finally it comes to

$$\begin{aligned} \int_{\Omega} \sigma \nabla(\dot{u}_d - h \nabla u_d) \cdot \nabla v \, dx &= - \int_{\partial\omega} [\sigma(h \cdot \nabla v) \partial_n u_d] + \int_{\partial\omega} [\sigma(\nabla u_d \cdot \nabla v) h_n] \\ &= (\sigma_1 - \sigma_2) \int_{\partial\omega} h_n (\nabla_{\tau} u_d) \cdot (\nabla_{\tau} v) = (\sigma_2 - \sigma_1) \int_{\partial\omega} \operatorname{div}_{\tau} (h_n \nabla_{\tau} u_D) v. \end{aligned}$$

Hence, the shape derivative $u'_d = \dot{u}_d - h \cdot \nabla u$ is solution of

$$\int_{\Omega} \sigma \nabla u'_d \cdot \nabla v = (\sigma_2 - \sigma_1) \int_{\partial\omega} \operatorname{div}_{\tau} (h_n \nabla_{\tau} u_d) v$$

and Green's formula enables us to get

$$- \int_{\Omega} \sigma \Delta u'_d v - \int_{\partial\omega} v [\sigma \partial_n u'_d] = (\sigma_2 - \sigma_1) \int_{\partial\omega} \operatorname{div}_{\tau} (h_n \nabla_{\tau} u_d) v.$$

This shows that u'_d satisfies $\Delta u'_d = 0$ on $\Omega \setminus \omega \cup \omega$ with the condition

$$[\sigma \partial_n u'_d] = (\sigma_1 - \sigma_2) \operatorname{div}_{\tau} (h_n \nabla_{\tau} u_d).$$

It remains to compute the jumps of u'_d . Since $\dot{u}_d \in H_0^1(\Omega)$, we have

$$[u'_d] = -h_n [\partial_n u_d], \quad (25)$$

and from the condition $[\sigma \partial_n u_d] = 0$ we get

$$[u'_d] = h_n \left(1 - \frac{\sigma_2}{\sigma_1}\right) \partial_n u_d^- = h_n \left(\frac{\sigma_1}{\sigma_2} - 1\right) \partial_n u_d^+.$$

This ends the proof of the shape differentiability of u_d . ■

In a similar way, we differentiate with respect to the shape the solution u_n of the Neumann problem and obtain

$$\begin{cases} \Delta u'_n &= 0 \text{ in } \Omega \setminus \bar{\omega} \text{ and in } \omega, \\ [u'_n] &= \frac{\sigma_1 - \sigma_2}{\sigma_1} \partial_n u_n^- V_n \text{ on } \partial\omega, \\ [\sigma \partial_n u'_n] &= (\sigma_1 - \sigma_2) \operatorname{div}_{\tau} (V_n \nabla_{\tau} u_n) \text{ on } \partial\omega, \\ \partial_n u'_n &= 0 \text{ on } \partial\Omega. \end{cases} \quad (26)$$

It satisfies the new normalization condition.

$$\int_{\partial\Omega} u'_n = 0.$$

3.3 Derivatives of the shape functionals

Lemma 3.2 (The Least Squares cost function) *One has:*

$$DJ_{LS}(\omega) \cdot V = -(\sigma_1 - \sigma_2) \int_{\partial\omega} \left(\frac{\sigma_1}{\sigma_2} \partial_n w^+ \partial_n u_d^+ + \langle \nabla_{\tau} u_d, \nabla_{\tau} w \rangle \right) V_n. \quad (27)$$

where the adjoint function w solves the equation

$$\begin{cases} -\operatorname{div}(\sigma w) &= 0 \text{ in } \Omega, \\ w &= \sigma_1 \partial_n u_d - g \text{ on } \partial\Omega, \end{cases} \quad (28)$$

Proof: One applies the derivation rule (see Proposition 5.4.18 in [8]) and from (20) to get

11

$$DJ_{LS}(\omega).V = \sigma_1 \int_{\partial\Omega} (\sigma_1 \partial_n u_d - g) \partial_n u'_d.$$

Then, writing Gauss formula in both $\Omega \setminus \bar{\omega}$ and ω , we get:

$$\int_{\partial\Omega} \partial_n u'_d w = \int_{\partial\omega} (\partial_n u'_d)^+ w - \partial_n w^+ (u'_d)^+, \quad (29)$$

$$\int_{\partial\omega} (\partial_n u'_d)^- w = \int_{\partial\omega} (u'_d)^- \partial_n w^-. \quad (30)$$

Plugging the jump conditions for both u'_d and w into (29), we obtain

$$\begin{aligned} \int_{\partial\Omega} \partial_n u'_d w &= \int_{\partial\omega} \left(\frac{\sigma_2}{\sigma_1} (\partial_n u'_d)^- + \frac{\sigma_2 - \sigma_1}{\sigma_1} \operatorname{div}_\tau (V_n \nabla_\tau u_d) \right) w \\ &\quad - \frac{\sigma_2}{\sigma_1} \partial_n w^- \left((u'_d)^- + \frac{\sigma_2 - \sigma_1}{\sigma_1} \partial_n u_d^- V_n \right). \end{aligned}$$

After an integration by part on $\partial\omega$ to get rid of the tangential divergence, we use (30) to obtain the claimed result. \blacksquare

For J_{DLS} , we prove in the same way

$$DJ_{DLS}(\omega).V = \frac{\sigma_1 - \sigma_2}{\sigma_1} \int_{\partial\omega} \left(\frac{\sigma_1}{\sigma_2} \partial_n w^+ \partial_n u_d^+ + \langle \nabla_\tau u_d, \nabla_\tau w \rangle \right) V_n,$$

where the adjoint function w solves the equation

$$\begin{cases} -\operatorname{div}(\sigma w) &= 0 \text{ in } \Omega, \\ \partial_n w &= u_d - f \text{ on } \partial\Omega, \end{cases}$$

The compatibility condition is satisfied thanks to the normalization (17). The adjoint has to be normalized for example as in (17).

Lemma 3.3 (The Kohn-Vogelius cost function) *One has*

$$DJ_{KV}(\omega).V = (\sigma_2 - \sigma_1) \int_{\partial\omega} \left[\frac{\sigma_1}{\sigma_2} (\partial_n u_d^+)^2 - \partial_n u_n^+ \right] + |\nabla_\tau u_d|^2 - |\nabla_\tau u_n|^2 \Big] V_n. \quad (31)$$

Proof: Since the state functions are differentiable, J_{KV} has also a shape derivative that is obtained by the chain rule. We get:

$$\begin{aligned} DJ_{KV}(\omega).V &= \sigma_1 \int_{\partial(\Omega \setminus \bar{\omega})} |\nabla(u_d - u_n)|^2 \langle V, n_{\Omega \setminus \bar{\omega}} \rangle + \sigma_1 \int_{\Omega \setminus \bar{\omega}} 2 \langle \nabla(u_d - u_n), \nabla(u'_d - u'_n) \rangle \\ &\quad + \sigma_2 \int_{\partial\omega} |\nabla(u_d - u_n)|^2 V_n + \sigma_2 \int_{\omega} 2 \langle \nabla(u_d - u_n), \nabla(u'_d - u'_n) \rangle \end{aligned}$$

Concerning the boundary terms, $V_n = 0$ on $\partial\Omega$ by construction, hence the integral on $\partial\Omega$ disappears. To express the term on $\partial\omega$, we decompose the gradient of the state functions into normal and tangential components and use the jump relations to get

$$\begin{aligned} &\int_{\partial\omega} [\sigma_2 |\nabla(u_d^- - u_n^-)|^2 - \sigma_1 |\nabla(u_d^+ - u_n^+)|^2] V_n \\ &= (\sigma_1 - \sigma_2) \int_{\partial\omega} \left[\frac{\sigma_1}{\sigma_2} (\partial_n(u_d^+ - u_n^+))^2 - |\nabla_\tau(u_d - u_n)|^2 \right] V_n. \end{aligned} \quad (32)$$

Concerning the volume term, we use the Gauss formula. Taking into account (15) and (16), we obtain: 12

$$\begin{aligned} \int_{\Omega \setminus \bar{\omega}} \langle \nabla(u_d - u_n), \nabla(u'_d - u'_n) \rangle &= - \int_{\partial\omega} \partial_n(u_d^+ - u_n^+) (u_d'^+ - u_n'^+) - \int_{\partial\Omega} \partial_n(u_d - u_n) u'_n, \\ \int_{\omega} \langle \nabla(u_d - u_n), \nabla(u'_d - u'_n) \rangle &= \int_{\partial\omega} \partial_n(u_d^- - u_n^-) ((u'_d)^- - (u'_n)^-). \end{aligned}$$

Using again the jump condition for both the state functions and their derivatives, we are led to

$$\begin{aligned} I &= \sigma_1 \int_{\Omega \setminus \bar{\omega}} \langle \nabla(u_d - u_n), \nabla(u'_d - u'_n) \rangle + \sigma_2 \int_{\omega} \langle \nabla(u_d - u_n), \nabla(u'_d - u'_n) \rangle \\ &= - \frac{\sigma_1}{\sigma_2} (\sigma_1 - \sigma_2) \int_{\partial\omega} (\partial_n(u_d^+ - u_n^+))^2 V_n - \sigma_1 \int_{\partial\Omega} \partial_n(u_d - u_n) u'_n. \end{aligned}$$

The term on $\partial\Omega$ involves u'_n defined by (26); to transform it into an integral on $\partial\omega$, we use the Gauss formula. We get in a first time

$$\int_{\partial\Omega} \partial_n u_d u'_n = \int_{\partial\omega} u_n'^+ \partial_n u_d^+ - u_d \partial_n u_n'^+ \text{ and } \int_{\partial\omega} (\partial_n u_n')^- u_d = \int_{\partial\omega} \partial_n u_d^- (u_n')^-.$$

Then incorporating the jump relation, we get:

$$\begin{aligned} \int_{\partial\Omega} \partial_n u_d u'_n &= \int_{\partial\omega} (u_n')^+ \partial_n u_d^+ - u_d \partial_n (u_n')^+, \\ &= \int_{\partial\omega} \frac{\sigma_2}{\sigma_1} \partial_n u_d^- \left((u_n')^- + \frac{\sigma_1 - \sigma_2}{\sigma_2} \partial_n u_n^- V_n \right) - u_d \partial_n (u_n')^+, \\ &= \int_{\partial\omega} \left(\frac{\sigma_2}{\sigma_1} (\partial_n u_n')^- - \partial_n (u_n')^+ \right) u_d + \frac{\sigma_1 - \sigma_2}{\sigma_1} \partial_n u_n^+ \partial_n u_d^- V_n, \\ &= \frac{\sigma_1 - \sigma_2}{\sigma_1} \int_{\partial\omega} -\operatorname{div}_\tau (V_n \nabla_\tau u_n) u_d + \frac{\sigma_1}{\sigma_2} \partial_n u_n^+ \partial_n u_d^+ V_n. \end{aligned}$$

Similar computations lead to

$$\int_{\partial\Omega} \partial_n u_n u'_n = \frac{\sigma_1 - \sigma_2}{\sigma_1} \int_{\partial\omega} -\operatorname{div}_\tau (V_n \nabla_\tau u_n) u_n + \frac{\sigma_1}{\sigma_2} (\partial_n u_n^+)^2 V_n.$$

We have obtained the new expression

$$\frac{\sigma_1}{\sigma_1 - \sigma_2} \int_{\partial\Omega} \partial_n(u_d - u_n) u'_n = \int_{\partial\omega} \frac{\sigma_1}{\sigma_2} \partial_n u_n^+ (\partial_n u_d^+ - \partial_n u_n^+) V_n - \operatorname{div}_\tau (V_n \nabla_\tau u_n) (u_d - u_n),$$

and after an integration by part on $\partial\omega$ which has no boundary, we obtain

$$I = -(\sigma_1 - \sigma_2) \int_{\partial\omega} \left(\frac{\sigma_1}{\sigma_2} \partial_n u_d^+ \partial_n (u_d^+ - u_n^+) + \langle \nabla_\tau u_n, \nabla_\tau (u_d - u_n) \rangle \right) V_n. \quad (33)$$

Adding (32) and (33), we obtain the claimed expression. ■

An important property of the Kohn-Vogelius cost function is that its gradient does not involve the derivative of the state function. This is a typical behavior of shape functionals of energy type: the same simplification also appears for the Dirichlet energy and for the compliance in linear elasticity. For numerical computations, it means that no adjoint state is needed for evaluating gradients.

Remark. Euler equations for both J_{LS} and J_{KV} are too complicated in the transmission case to give useful information. In particular, one cannot deduce easily that the criteria vanish at any critical shape. Such a property is closely connected to the well-posedness of the criteria and to the identifiability question that are to our best knowledge still open. Nevertheless, let us mention the work [5] where Eppler and Harbrecht deduce, in the perfectly conducting case, the Euler equation associated to J_{KV} implies that $J_{KV}(\omega^*) = 0$ for any local minimizer ω^* via a unique continuation argument .

4 Numerical experiments

4.1 Computing the state function

In this paragraph, we describe how the state functions (u_d, u_n and w) are computed. We use the boundary element method since only boundary values of the state function (and of their derivatives) are needed to evaluate the shaping functions and their derivatives.

We introduce $\Gamma(x, y)$ the fundamental solution of the Laplacian given in dimension two by:

$$\Gamma(x, y) = \frac{1}{2\pi} \ln(|x - y|).$$

Taking into account the orientation of the normal to $\partial\omega$, the boundary representation formula for any u harmonic in $\Omega \setminus \omega$ writes $\forall x \in \partial\Omega \cup \partial\omega$:

$$\frac{1}{2}u(x) = \int_{\partial\Omega} \partial_n \Gamma(x, y) u(y) - \int_{\partial\omega} \partial_n \Gamma(x, y) u(y) - \int_{\partial\Omega} \Gamma(x, y) \partial_n u(y) + \int_{\partial\omega} \Gamma(x, y) \partial_n u(y). \quad (34)$$

We also have for any u harmonic in ω :

$$\forall x \in \partial\omega \quad \frac{1}{2}u(x) = \int_{\partial\omega} \partial_n \Gamma(x, y) u(y) - \int_{\partial\omega} \Gamma(x, y) \partial_n u(y). \quad (35)$$

Let us explain how to compute u_d . The unknowns are $(u_d)|_{\partial\omega}$, $(\partial_n u_d)|_{\partial\Omega}$ and $(\partial_n u_d)|_{\partial\omega}^+$. First, using the jump condition and (35), we notice that

$$\forall x \in \partial\omega, \int_{\partial\omega} \Gamma(x, y) \partial_n u^+ = \frac{\sigma_2}{\sigma_1} \left[-\frac{1}{2}u(x) + \int_{\partial\omega} \partial_n \Gamma(x, y) u(y) \right]. \quad (36)$$

Injecting this relation into (34), we obtain for $x \in \partial\omega$:

$$\left[\frac{\sigma_1 + \sigma_2}{2\sigma_1} u(x) + \frac{\sigma_1 - \sigma_2}{\sigma_1} \int_{\partial\omega} \partial_n \Gamma(x, y) u(y) \right] + \int_{\partial\Omega} \Gamma(x, y) \partial_n u(y) = \int_{\partial\Omega} \partial_n \Gamma(x, y) f(y). \quad (37)$$

Now, from Green's formula in ω and $d(\partial\omega, \partial\Omega) > d_0$, we notice for $x \in \partial\Omega$

$$\frac{\sigma_1}{\sigma_2} \int_{\partial\omega} \Gamma(x, y) \partial_n u(y)^+ = \int_{\partial\omega} \partial_n \Gamma(x, y) u(y),$$

that gives in (34),

$$\frac{\sigma_2 - \sigma_1}{\sigma_1} \int_{\partial\omega} \partial_n \Gamma(x, y) u(y) - \int_{\partial\Omega} \Gamma(x, y) \partial_n u(y) = \frac{1}{2}f(x) - \int_{\partial\Omega} \partial_n \Gamma(x, y) f(y). \quad (38)$$

To write the corresponding integral equations, we use the material developed by the theory of "single and double layer potentials". At this end, we introduce the following single and the double layer operators with the boundaries $\partial\Omega$ and $\partial\omega$:

$$\begin{aligned} S_{\partial\Omega\partial\omega}u(x) &:= \int_{\partial\Omega} \Gamma(x,y)u(y) ds_y, \quad x \in \partial\omega; \\ S_{\partial\omega\partial\Omega}u(x) &:= \int_{\partial\omega} \Gamma(x,y)u(y) ds_y, \quad x \in \partial\Omega; \\ K_{\partial\Omega\partial\omega}u(x) &:= \int_{\partial\Omega} \partial_n\Gamma(x,y)u(y) ds_y, \quad x \in \partial\omega; \\ K_{\partial\omega\partial\Omega}u(x) &:= \int_{\partial\omega} \partial_n\Gamma(x,y)u(y) ds_y, \quad x \in \partial\Omega. \end{aligned}$$

We also denote

$$\begin{aligned} S_{\Omega}u(x) &:= \int_{\partial\Omega} \Gamma(x,y)u(y) ds_y, \quad x \in \partial\Omega; \quad \text{and} \quad K_{\Omega}u(x) := \int_{\partial\Omega} \partial_n\Gamma(x,y)u(y) ds_y, \quad x \in \partial\Omega. \\ S_{\omega}u(x) &:= \int_{\partial\omega} \Gamma(x,y)u(y) ds_y, \quad x \in \partial\omega; \quad \text{and} \quad K_{\omega}u(x) := \int_{\partial\omega} \partial_n\Gamma(x,y)u(y) ds_y, \quad x \in \partial\omega. \end{aligned}$$

Let A be the matricial operator defined by

$$A = \begin{bmatrix} \frac{1}{2}I + \mu K_{\omega} & \frac{\sigma_1}{\sigma_2 + \sigma_1} S_{\partial\Omega\partial\omega} \\ \frac{\sigma_1 - \sigma_2}{\sigma_1} K_{\partial\omega\partial\Omega} & S_{\Omega} \end{bmatrix} \quad (39)$$

on $H^{1/2}(\partial\omega) \times H^{-1/2}(\partial\Omega)$. Then, the equations (37 – 38) can be written under the following form :

$$A \begin{bmatrix} (u_d)|_{\partial\omega} \\ (\partial_n u_d)|_{\partial\Omega} \end{bmatrix} = \begin{bmatrix} \frac{\sigma_1}{\sigma_2 + \sigma_1} K_{\partial\Omega\partial\omega} f \\ \left(-\frac{1}{2}I + K_{\Omega} \right) f \end{bmatrix}. \quad (40)$$

The quantity $(\partial_n u_d)^+$ is then found after solving (36):

$$S_{\omega}(\partial_n u_d)|_{\partial\omega}^+ = \frac{\sigma_2}{\sigma_1} \left[-\frac{1}{2}I + K_{\omega} \right] u_d(x)|_{\partial\omega}. \quad (41)$$

We now state a well-posedness result for these equations.

Theorem 4.1 *The linear system of integral equation (40) has a unique solution.*

Proof: We begin to show that the adjoint operator A^* is injective. Since the boundaries are bounded, the adjoint operator writes

$$A^* = \begin{bmatrix} \frac{1}{2}I + \mu K_{\omega}^* & \frac{\sigma_1 - \sigma_2}{\sigma_1} K_{\partial\Omega\partial\omega}^* \\ \frac{\sigma_1}{\sigma_2 + \sigma_1} S_{\partial\omega\partial\Omega} & S_{\Omega} \end{bmatrix}. \quad (42)$$

Let $(u, v) \in H^{1/2}(\partial\omega) \times H^{-1/2}(\partial\Omega)$ be a solution to the homogenous equation $A^*(u, v) = 0$ and define a potential W by

$$W(x) = \frac{\sigma_1}{\sigma_2 + \sigma_1} \int_{\partial\omega} \Gamma(x,y)u(y)ds(y) + \int_{\partial\Omega} \Gamma(x,y)v(y)ds(y), \quad x \in \mathbb{R}^d. \quad (43)$$

Let us show that $W = 0$. It is obvious that the function W satisfies $\Delta W = 0$ on $\mathbb{R}^d \setminus (\partial\omega \cup \partial\Omega)$. From the equation corresponding to the second line of A^* , we see that $W|_{\partial\Omega} = 0$. Let us study the jump conditions on $\partial\omega$. By the properties of the single layer potential, $[W] = 0$ on $\partial\omega$. Now, let us prove that $[\sigma\partial_n W] = 0$ on $\partial\omega$. We have

$$\sigma_1\partial_n W_+ = \sigma_1 \left(\frac{\sigma_1}{\sigma_1 + \sigma_2} \left(\frac{1}{2} + K_\omega^* \right) u + K_{\partial\Omega\partial\omega}^* v \right)$$

and

$$\sigma_2\partial_n W_- = \sigma_2 \left(\frac{\sigma_1}{\sigma_1 + \sigma_2} \left(-\frac{1}{2} + K_\omega^* \right) u + K_{\partial\Omega\partial\omega}^* v \right).$$

Hence,

$$\sigma_1\partial_n W_+ - \sigma_2\partial_n W_- = \sigma_1 \left(\left(\frac{1}{2}I + \mu K_\omega^* \right) u + \frac{\sigma_1 - \sigma_2}{\sigma_1} K_{\partial\Omega\partial\omega}^* v \right).$$

This corresponds to the first line of $A^*(u, v) = 0$. Hence, W is solution of a Poisson equation (2) with homogeneous Dirichlet boundary conditions. By uniqueness of the solution of the homogenous Dirichlet problem, we get $W = 0$ in Ω .

We are ready to show that $W = 0$ in Ω implies $u = v = 0$. It is straightforward to see that $u = 0$. Indeed, since $W = 0$ in Ω , we have $[\partial_n W] = 0$ on $\partial\omega$ and this gives $[\partial_n W] = \sigma_1 u / (\sigma_1 + \sigma_2)$ on $\partial\omega$. Hence, we have $u = 0$. From the second line of $A^*(u, v) = 0$, we see that $S_\Omega v = 0$ on $\partial\Omega$. Since the single layer potential operator $S_\Omega : H^{s-1}(\partial\Omega) \mapsto H^s(\partial\Omega)$, $\forall s$ is an isomorphism, we then get $v = 0$. The injectivity of A^* is proved. Since $2A = I + C$ where C is a compact operator, the Fredholm alternative enables us to conclude the invertibility of A . \blacksquare

Concerning u_n , the unknowns are $(u_n)_{\partial\Omega}$, $(u_n)_{\partial\omega}$ and $(\partial_n u_n)_{\partial\omega}^+$. Similar computations lead to:

$$\begin{bmatrix} \frac{1}{2}I + \mu K_\omega & -\frac{\sigma_1}{\sigma_2 + \sigma_1} K_{\partial\Omega\partial\omega} \\ \frac{\sigma_2 - \sigma_1}{\sigma_1} K_{\partial\omega\partial\Omega} & -\frac{1}{2}I + K_\Omega \end{bmatrix} \begin{bmatrix} (u_n)_{\partial\omega} \\ (u_n)_{\partial\Omega} \end{bmatrix} = \begin{bmatrix} -\frac{\sigma_1}{\sigma_2 + \sigma_1} S_{\partial\Omega\partial\omega} g \\ S_\Omega g \end{bmatrix}. \quad (44)$$

Then, $(\partial_n u_n)_{\partial\omega}^+$ is given by

$$S_{\partial\omega\partial\omega}(\partial_n u_n)_{\partial\omega}^+ = \frac{\sigma_2}{\sigma_1} \left[-\frac{1}{2}I + K_\omega \right] u_n(x)_{\partial\omega}. \quad (45)$$

Concerning the existence and uniqueness of the solution of (44), we have the following result

Proposition 4.2 *If we impose the normalization*

$$\int_{\partial\Omega} u_n ds = \int_{\partial\Omega} f,$$

then there exists one unique pair $((u_n)_{\partial\omega}, (u_n)_{\partial\Omega})$ solution of (44).

Proof: Set

$$B = \begin{bmatrix} \frac{1}{2}I + \mu K_\omega & -\frac{\sigma_1}{\sigma_2 + \sigma_1} K_{\partial\Omega\partial\omega} \\ \frac{\sigma_2 - \sigma_1}{\sigma_1} K_{\partial\omega\partial\Omega} & -\frac{1}{2}I + K_\Omega \end{bmatrix} \quad (46)$$

the operator defined on $H^{1/2}(\partial\omega) \times H_{\diamond}^{1/2}(\partial\Omega)$ where

16

$$H_{\diamond}^{1/2}(\partial\Omega) = \left\{ \phi \in H^{\frac{1}{2}}(\partial\Omega) : \int_{\partial\Omega} \phi dS = 0 \right\}.$$

The adjoint B^* can be written under the form

$$B^* = \begin{bmatrix} \frac{1}{2}I + \mu K_{\omega}^* & \frac{\sigma_2 - \sigma_1}{\sigma_1} K_{\partial\Omega\partial\omega}^* \\ -\frac{\sigma_1}{\sigma_2 + \sigma_1} K_{\partial\omega\partial\Omega}^* & -\frac{1}{2}I + K_{\Omega}^* \end{bmatrix} \quad (47)$$

In a first step, we begin to show that B^* is injective. As we did before, we define the adequate potential: for $x \in \mathbb{R}^d$

$$Z(x) = -\frac{\sigma_1}{\sigma_1 + \sigma_2} \int_{\partial\omega} \Gamma(x, y) u(y) ds(y) + \int_{\partial\Omega} \Gamma(x, y) v(y) ds(y), .$$

We can see that Z is a harmonic function $\mathbb{R}^d \setminus (\partial\omega \cup \partial\Omega)$, satisfying $\partial_n Z = 0$. Furthermore, $[Z] = 0$ and a straightforward calculation shows that $[\sigma \partial_n Z] = 0$ on $\partial\omega$. Hence, Z is a constant function in Ω . Writing $[\partial_n Z] = 0$ on $\partial\omega$, we get easily $u = 0$ and then $(-\frac{I}{2} + K_{\Omega}^*)v = 0$. Since the operator $\lambda I - K_{\Omega}^*$ is one to one on $H_{\diamond}^{1/2}(\partial\Omega)$, we deduce that $v = 0$. We conclude the proof thanks to the Fredholm alternative. ■

4.2 The optimization procedure and numerical results

For the discretization of $\partial\omega$, we restrict ourselves to the case where $\partial\omega$ is star-shaped with respect to some point. This is admissible since the convergence of the iterative reconstruction by conformal mapping is only achieved for inclusion close to disks close to concentric disks. The advantage of star-shaped inclusions with respect to the origin for numerical reconstruction is the possibility to use a polar representation of the boundary $\partial\omega$. This allows to obtain an expression of the shape derivatives in terms of the boundary representation.

Another possibility to discretize the evolution of the shape is to use the level set method as in [10]. However, the main advantage of the level set approach is its flexibility to the topology of the objective. We have assumed from the beginning of the paper that the inclusion ω is simply connected in order to have a simple conformal model. This assumption as well as the restriction to bi-dimensional cases are required only for the computation of an adequate starting shape. The shape calculus presented in Section 3 is also valid without these restrictions.

We consider an inclusion with boundary $\partial\omega$ that can be parametrized as:

$$\partial\omega = \left\{ r(t) \begin{pmatrix} \cos t \\ \sin t \end{pmatrix}, t \in (0, 2\pi) \right\}$$

where $r(t)$ is a \mathcal{C}^2 function, 2π - periodic and without double point. For the numerical resolution, we approximate it by its truncated Fourier series

$$r_n(t) = \left(a_0 + \sum_{k=1}^n a_k \cos kt + b_k \sin kt \right).$$

The unknowns defining the geometry are the Fourier coefficients (a_i, b_i) . The discrete optimization problem is written with these coefficients as variables. Hence, the deformation field V is chosen as $V(t) = h_n(t)(\cos t, \sin(t))$ with :

$$h_n(t) = \left(a(V)_0 + \sum_{k=1}^n a(V)_k \cos kt + b(V)_k \sin kt \right).$$

Its normal component is computed easily and one gets

17

$$V_n(t) = \frac{h(t)r(t)}{\sqrt{r(t)^2 + r'(t)^2}}.$$

Using lemmata (3.3) and (3.2), we obtain :

$$DJ_{KV}(\omega).h = (\sigma_2 - \sigma_1) \int_0^{2\pi} \left[\frac{\sigma_1}{\sigma_2} ((\partial_n u_d^+)^2 - (\partial_n u_n^+)^2) + |\nabla_\tau u_d|^2 - |\nabla_\tau u_n|^2 \right] hr; \quad (48)$$

$$DJ_{LS}(\omega).h = (\sigma_2 - \sigma_1) \int_0^{2\pi} \left(\frac{\sigma_1}{\sigma_2} \partial_n w^+ \partial_n u_d^+ + \langle \nabla_\tau u_d, \nabla_\tau w \rangle \right) hr. \quad (49)$$

These formulae provides the discretized gradient DJ_{KV} and DJ_{LS} in all directions. The analysis of the Newton method for the perfectly conducting inclusion case is performed in [5]. The need of regularization suggests to use Levenberg-Maquardt or other quasi-Newton algorithms. Hence, we use the BFGS algorithm to solve the optimization problem. This quasi-Newton method is well adapted to such a problem.

The integral equations (40- 45) are solved by the collocation method; let us emphasize that the boundaries are approximated by broken lines with more vertices than the number of Fourier modes. The $\nabla_\tau u_d$ and $\nabla_\tau u_n$ quantities can be computed by differentiating the piecewise linear representation of $(u_d)|_{\partial\omega}$ and $(u_n)|_{\partial\omega}$ respectively. To make sense, the discretization of the unknown functions u and $\partial_n u$ should be at least P_1 . In the following numerical experiments, we used a ratio of six. This is an efficient regularization method for this problem.

First domain. We consider the domain defined by:

$$\partial\omega = \left\{ \begin{pmatrix} 0.1 + 0.5 \cos(t) + 0.1 \cos(4t) \\ 0.5 \sin(t) + 0.1 \cos(4t) \end{pmatrix}, t \in [0, 2\pi] \right\}$$

We use simulated data corresponding to the Dirichlet data $f(t) = \sin t$. For the test with noisy data, we perturbed the Neumann data by gaussian noise with fixed amplitude. In these tests, the conductivities are chosen as $\sigma_1 = 1$ and $\sigma_2 = 3$.

First, we present in Figure 1 the reconstruction obtained with the three methods we presented in the work: the conformal mapping method with numerical extension of the result of the fixed point algorithm, then the minimization of the Least Squares fitting and Kohn-Vogelius criteria. In both optimization methods, we used as starting point the circle obtained by the conformal mapping method and 13 Fourier modes. In Figure 1, we present this approximating disk. It will not appear in the next results even if it is used as starting point for the minimization. This explains that in the convergence histories we present the starting has already an error of order 10^{-3} and that only a few iterations are needed.

In Figure 2, we compare the merits of J_{LS} and J_{KV} for exact data with 25 modes this time. We present the logarithmic error with respect to the number of iterations. Both methods seem to be of equivalent quality.

As soon as data are noised, the Kohn-Vogelius criterion becomes more robust than the Least Squares fitting. This is illustrated in Figure 3. Another practical reason to prefer the Kohn-Vogelius criterion is the running time required to end the iterations. Our experience leads to at least a 2 ratio in favor of J_{KV} with the same codes for solving the states. The explanation lays in the line search for BFGS where Wolfe's rule is satisfied more easily for J_{KV} .

Second domain. Now, we consider the reference kite shaped domain defined by:

$$\partial\omega = \left\{ \begin{pmatrix} 0.1 + 0.3 \cos(t) + 0.2 \cos(2t) \\ 0.4 \sin(t) \end{pmatrix}, t \in [0, 2\pi] \right\}$$

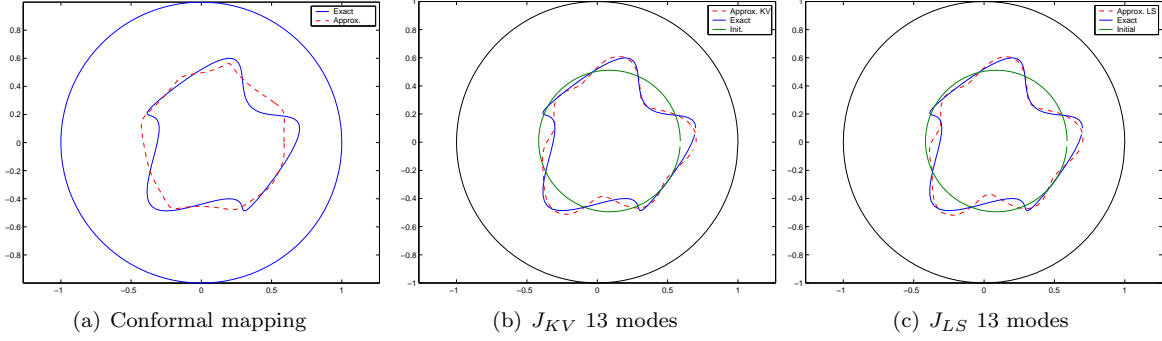


Figure 1: Conformal mapping extension versus shape gradients.

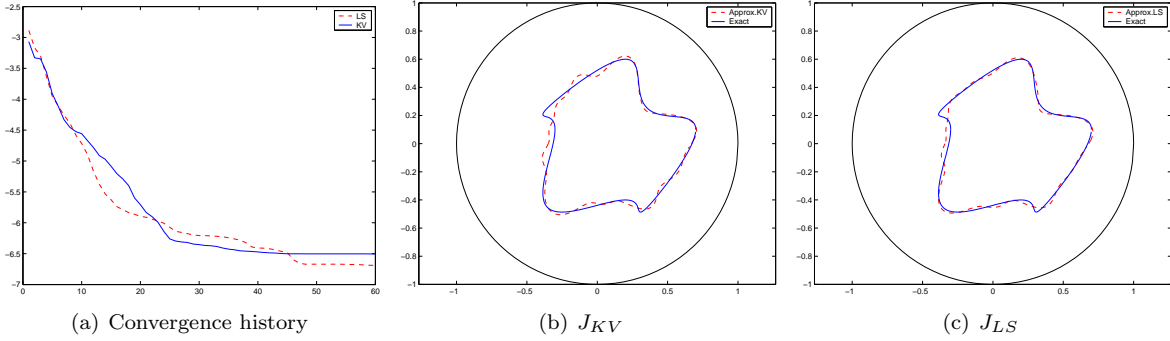


Figure 2: Comparison of the criteria with 25 modes .

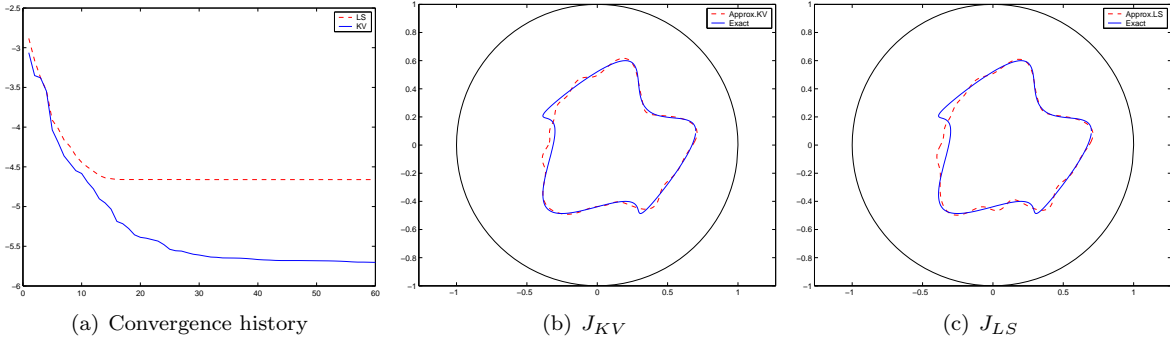


Figure 3: Comparison of the criteria with noised data (1%) and 25 modes

We use simulated data corresponding to the Dirichlet data $f(t) = \cos t$. For the test with noisy data, we still perturb the Neumann data by gaussian noise with fixed amplitude. We keep the same conductivities. In Figure 4, we present the results obtained by the different methods with 25 Fourier modes. The obtained reconstruction is not as satisfactory as in Figure 2. The difficulty comes from the pronounced concavity of the kite shape. In Figure 5, we present the noisy case. Both methods start from the same point. The Kohn-Vogelius criterion leads to more robust reconstruction as emphasized in the convergence history.

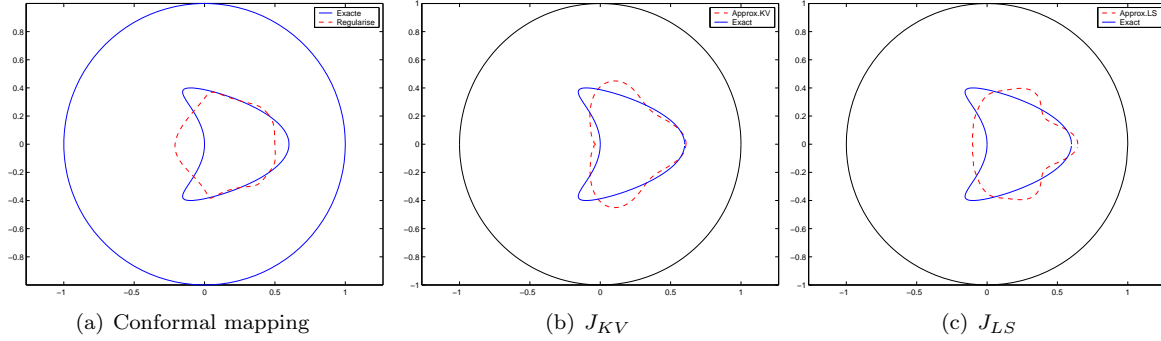


Figure 4: Conformal mapping extension versus shape gradients.

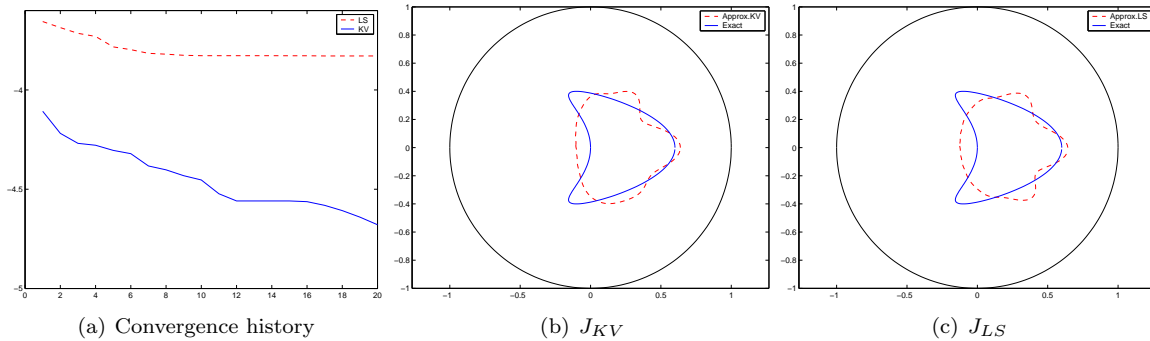


Figure 5: Comparison of the criteria with noised data (3%) and 25 modes

References

- [1] I. Akduman, and R. Kress. Electrostatic imaging via conformal mapping, *Inverse Problems* 18 (2002) 1659-1672.
- [2] G. Alessandrini, and E. Rosset. Volume bounds of inclusions from physical EIT measurements *Inverse Problems* 20 (2004) 575-588.
- [3] H. Ammari, and H. Kang. Reconstruction of small inhomogeneities from Boundary Measurements. *Lecture Notes in Mathematics* 1846.
- [4] M. Dambrine, and D. Kateb. Conformal mapping and inverse conductivity problem with one measurement, to appear in *ESAIM: Control Optimisation and Calculus of Variations*.
- [5] K. Eppler, and H. Harbrecht. A regularized Newton method in electrical impedance tomography using Hessian information, *Control and Cybernetics* (34) 2005, 203-225.
- [6] H. Haddar, and R. Kress. Conformal mappings and inverse boundary value problems. *Inverse Problems* 21 (2005) 935-953.
- [7] P. Henrici. *Applied and computational complex analysis, Vol 1,3*. John Wiley & Sons, 1986
- [8] A. Henrot, and M. Pierre. *Variation et optimisation de formes*. Springer Mathématiques et Applications, Vol 48, 2005
- [9] F. Hettlich, and W. Rundell. The determination of a discontinuity in a conductivity from a single boundary measurement, *Inverse Problems* 14 (1998) 67-82.

- [10] K.Ito, K.Kunisch, and Z.Li. Level-set function approach to an inverse interface problem, *Inverse Problems* 17 (2001) 1225-1242.
- [11] H. Kang, J.K. Seo, and D. Sheen. The inverse conductivity problem with one measurement: stability and estimation of size. *SIAM J. Math. Anal.* 28, N-6, pp 1389-1405 (1997).
- [12] O. Pantz. Sensibilité de l'équation de la chaleur aux sauts de conductivité, *C.R. Acad. Sci. Paris, Ser. I* 341 (2005).
- [13] J.R. Roche, and J. Sokolowski. Numerical methods for shape identification problems, *Control and Cybernetics* (25) 1996, 867-894.